Removal of Total Dissolved Solids from Reverse Osmosis Concentrates from a Municipal Wastewater Reclamation Plant by Aerobic Granular Sludge

Do-Hyung Kim

Sangjin Park

Yeomin Yoon
University of South Carolina - Columbia, yoony@cec.sc.edu

Chang Min Park

Removal of Total Dissolved Solids from Reverse Osmosis Concentrates from a Municipal Wastewater Reclamation Plant by Aerobic Granular Sludge

Do-Hyung Kim [1,†], Sangjin Park [2,†], Yeomin Yoon [3] and Chang Min Park [4,*]

1 Korea Environmental Industry & Technology Institute, 215 Jinheungno, Eunpyeong-gu, Seoul 03367, Korea; dhkim1979@naver.com
2 Aquatic Ecosystem Conservation Division, Water Environment Management Bureau, Ministry of Environment, Government Complex-Sejong, 11 Doum 6-ro, Sejong-Special Self-Governing City 30103, Korea; psjin@korea.kr
3 Department of Civil and Environmental Engineering, University of South Carolina, 300 Main Street, Columbia, SC 29208, USA; yoony@cec.sc.edu
4 Department of Environmental Engineering, Kyungpook National University, 80 Daehak-ro, Buk-gu, Daegu 41566, Korea
* Correspondence: cmpark@knu.ac.kr; Tel.: +82-53-950-6581; Fax: +82-53-950-6579
† These authors contributed equally to the current work.

Abstract: Reverse osmosis (RO) has been widely utilized in water reclamation plants and produces a concentrated brine (or reject) stream as a by-product. RO concentrates (ROC) contain vast quantities of salts and dissolved organic matter, such as biomass and humic-like substances, which hinder biological wastewater treatment (such as biological nitrogen removal). In this study, we cultivated granular sludge in an aerobic sequencing batch reactor to treat municipal wastewater with an organic loading rate of 2.1–4.3 kgCOD/m^3 day at room temperature (25 °C), and remove total dissolved solids (TDS) from ROC by biosorption, with aerobic granular sludge as a novel biosorbent. The results of the kinetic experiments demonstrated that TDS removal by aerobic granular sludge was more rapid than that by other coagulants and adsorbents (i.e., calcium hydroxide, polyaluminum chloride, activated sludge, powdered activated carbon, granular activated carbon, and zeolite) under optimal treatment conditions. The biosorption of TDS on the aerobic granular sludge was well-modeled by the Lagergren first-order model, with a maximum biosorption capacity of 1698 mg/g. Thus, aerobic granular sludge could be effective as a regenerable biosorbent for removing the TDS in ROC from municipal wastewater.

1. Introduction

Current and projected future water shortages constitute a major threat to life on Earth, including humans, and many aspects of agriculture, such as irrigation [1]. In recent years, rapidly expanding populations and water quality degradation have reduced access to freshwater resources from rivers and lakes. It is estimated that, as of 2016, more than 1.8 billion people worldwide are unable to access a safe drinking water supply, and can only reach unsafe water sources [2]. Two-thirds of the global population could face severe water scarcity by 2025 [3]. The limited access to clean water and poor sanitation increases disease burden, particularly infectious diarrhea and enteric illnesses. Annual global child mortalities (younger than 5 years) are associated with water- and sanitation-related

diseases, most of which are preventable through suitable water treatment [4]. Approximately 3% of the Earth's water is fresh, less than 1% of which is usable by humans [5]; therefore, a promising approach to reduce water scarcity is to separate salt from sea and inland saline water in a process called desalination.

The most common methods of desalination are reverse osmosis (RO) and conventional thermal technologies, such as multi-stage flash (MSF) distillation. RO membranes push water molecules from saline water to the less saline area by applying a hydraulic pressure ($\triangle P$) greater than the osmotic pressure ($\triangle \pi$) across a semi-permeable membrane, while thermal technologies desalinate saline water by evaporation and condensation [6,7]. Deciding on a suitable treatment technology is dependent on the feed water salinity, water recovery rate, total space available, and the cost of operation. Currently, RO is the leading desalination technology using a membrane as it has a small carbon footprint, lower energy consumption than the thermal alternatives, and better compatibility with other treatment processes [8,9]. RO processes have been employed in full-scale drinking water production, tertiary wastewater treatment, and water reclamation [9]. However, a hyper-saline brine concentrate can be generated as a waste product during these processes [10]. The direct disposal of RO concentrates (ROC) into seawater was considered to be the most economical disposal method; however, it could pose a potentially serious threat to coastal and marine ecosystems. In addition, legal and regulatory concerns are being raised over the long-term environmental effects of this disposal method.

Designing sustainable management strategies for ROC is a key factor in the development of water/wastewater reclamation and recycling. ROC contains vast quantities of dissolved salts, effluent organic matter (EfOM), such as biomass (polysaccharides) and humic-like substances, and recalcitrant organics, which cannot be easily degraded by biological wastewater treatment [11,12], and limits its application in water recycling [13]. Considerable attention has been devoted to overcoming the environmental concerns associated with ROC management. This includes the zero liquid discharge (ZLD) process, membrane distillation and dewvaporation, and high-efficiency RO (HERO^{TM}) [14,15]. The major challenges of those techniques are their high capital investment and solid/liquid waste generation that requires special handling.

Conventional treatment processes, such as coagulation/flocculation and adsorption, have been widely investigated for removing EfOM from ROC due to their low cost and simplicity [16,17]. Dialynas et al. [18] evaluated these conventional processes using alum ($Al_2(SO_4)_3 \cdot 18H_2O$), ferric chloride ($FeCl_3$), and granular activated carbon (GAC) for the treatment of ROC of membrane bioreactor (MBR) effluent. Their results suggested that GAC and ferric chloride were promising as coagulants as their removal efficiencies of dissolved organic carbon (DOC) were higher (91.3% and 52%, respectively) than the alum tested (42%) [19]. Bagastyo et al. [16] reported that iron removed a wider molecular weight (MW) range of organics in ROC from coastal and inland streams than alum under optimal coagulation conditions (1.5 mM Al at pH 5 and 1.48 mM Fe at pH 5). Zhou et al. [17] found that coupling pretreatment with ferric chloride could remove a large quantity of heavy MW organics from ROC that are highly resistant to the subsequent advanced oxidation process (95% removal by the $FeCl_3/UVC/TiO_2$ system).

Recently, aerobic granulation technology has received much attention for treating wastewater that contains substances, such as organics, toxicants, and xenobiotics, due to its excellent settleability and high porosity [20–24]. Bassin et al. [23] investigated the ammonium adsorption properties of aerobic granular sludge. Their results showed that the aerobic granular sludge had a much greater adsorption capacity (0.9–1.7 mg NH4-N/g VSS) than activated sludge (AS) and anammox granules. Liu et al. [24] showed that the aerobic granules had excellent Cd(II) adsorption capability (maximum Cd(II) biosorption capacity: 566 mg/g), which was highly dependent on the initial Cd(II) and granules concentrations. However, very little is known regarding the feasibility of aerobic granular sludge as a novel type of biosorbent for the removal of organics from ROC [25]. Therefore, the objectives of this study were to evaluate aerobic granular sludge, composed of self-immobilized cells, as a novel biosorbent for ROC pretreatment and model the biosorption of total dissolved solids (TDS)

by the aerobic granular sludge. Conventional treatment processes (i.e., coagulation with calcium hydroxide ($Ca(OH)_2$) and polyaluminum chloride (PACl), and adsorption with AS, powdered activated carbon (PAC), granular activated carbon (GAC), and zeolite) were also applied to compare their ROC treatabilities.

2. Materials and Methods

2.1. Material Preparation

ROC was collected from the RO treatment process of a municipal wastewater reclamation plant in Pohang, South Korea that allows the reuse of secondary sewage effluent. The received ROC were stored in a refrigerator (4 °C) and warmed to room temperature (25 °C) prior to use. The characteristics of the ROC samples are summarized in Table 1. The aerobic granular sludge was cultivated in an aerobic sequencing batch reactor (SBR) that treats municipal wastewater with an organic loading rate of 2.1–4.3 kgCOD/m^3 day at room temperature prior to use as a biosorbent (Figure 1). The SBR was made from Plexiglas with an internal diameter of 12 cm, a total height of 110 cm, and a working volume of 9.1 L. The SBR was aerated with fine bubbles that were discharged into the bottom at a superficial air velocity of 0.004–0.013 m/h [26]. Inorganic coagulants, including $Ca(OH)_2$ and PACl (17% *w/w*), and commercial adsorbents, including coal-based PACl (Norit SA Super, Amersfoort, Netherlands), GAC (Norit 1020, Amersfoort, Netherlands), and zeolite (Daejung Chemicals & Metals Co., Ltd., Inchon, Gyeonggi-do, Korea), did not undergo further purification. AS was obtained from a municipal wastewater treatment process. Deionized (DI) water (18.2 MΩ·cm) was produced using a Barnstead DI water system. All chemicals were of analytical-reagent grade.
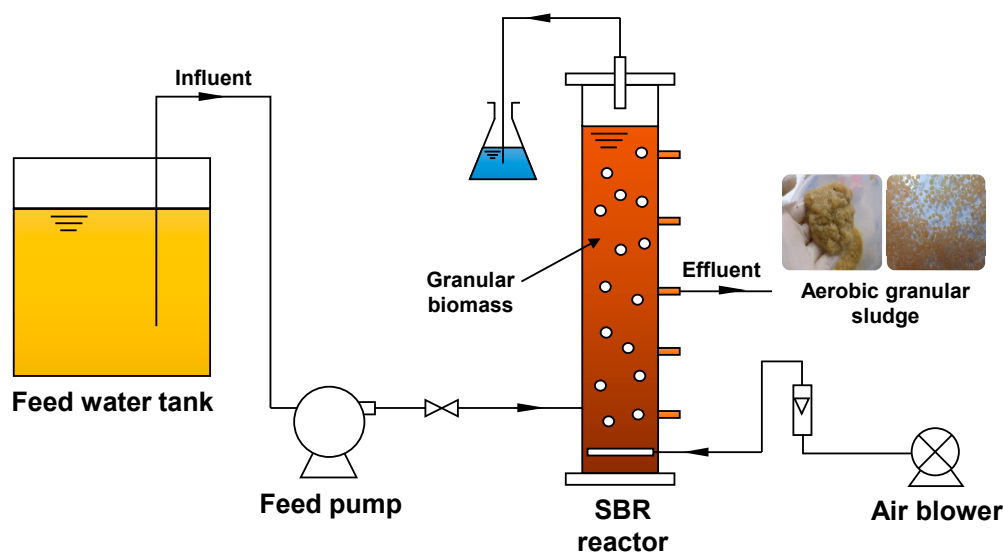

Figure 1. Schematic diagram of experimental setup for the sequencing batch reactor (SBR).

Table 1. Characteristics of the ROC sample from municipal wastewater reclamation plant.

Parameters	Values
pH	7.99 ± 0.53
Alkalinity (mg/L)	366 ± 55.3
BOD_5 (mg/L)	387 ± 47.5
NO_3^-–N (mg/L)	75.0 ± 5.98
NH_3^-–N (mg/L)	4.99 ± 0.91
PO_4^{3-}–P (mg/L)	1.96 ± 0.64
TDS * (mg/L)	2043 ± 216

Table 1. *Cont.*

Parameters	Values
Cations (mg/L)	
K^+	52.3 ± 14.1
Na^+	230 ± 26.3
Ca^{2+}	302 ± 54.7
Mg^{2+}	72.4 ± 20.8
Anions (mg/L)	
Cl^-	648 ± 36.9
HCO_3^-	348 ± 30.2
SO_4^{2-}	320 ± 23.5

* TDS: total dissolved solid.

2.2. Characterization of Aerobic Granular Sludge

After cultivation in an SBR that receives municipal wastewater, the aerobic granular sludge was fixed with 2.5% glutaraldehyde in a phosphate-buffered saline solution. The aerobic granular sludge was then stained using the sequence and wavelengths proposed by Chen et al. [27], with SYTO 63, SYTO blue, fluorescently−labeled lectin concanavalin A (Con A), Nile red, and fluorescein isothiocyanate (FITC) (Molecular Probes, Eugene, OR, USA) for nucleic acid, dead cells, α-D-glucopyranose polysaccharides, lipid, and proteins, respectively [28–31]. After fluorescent staining, the frozen aerobic granular sludge samples were cut on a cryostat (Microm HM 525, Thermo scientific, Bremen, Germany) in preparation for confocal laser scanning microscopy (CLSM; FV1000-IX81, Olympus, Tokyo, Japan) images to analyze the internal structure (spatial distribution profiles) using the Leika confocal software (version 2.5, Leica Microsystems, Heidelberg, Germany) in Figure 2. The nitrogen adsorption–desorption isotherms of the coagulants and adsorbents were recorded with an ASAP 2020 (Micromeritics Ins., Norcross, GA, USA) [32]. The samples were degassed in situ at 573 K and 1.33×10^{-6} bar for 6 h before analysis. The effective specific surface areas of the coagulants/adsorbents were determined using the Brunauer-Emmett-Teller (BET) method.

After the coagulation and adsorption experiments, TDS-adsorbed aerobic granular sludge (0, 2000, 3000, and 4000 mg/L) was dried at 105 °C overnight so it could be characterized. Interactions between TDS and aerobic granular sludge were examined with scanning (SEM, JSM-6500F, JEOL Ltd., Tokyo, Japan) and transmission electron microscopes (TEM, JEM-1010, JEOL Ltd., Tokyo, Japan) at 80 kV. X-ray photoelectron spectroscopy (XPS) of TDS-sorbed aerobic granular sludge was conducted using an ESCALAB 201 (VG Scientific Co., Manchester, UK) electron spectrophotometer to determine the chemical compositions and binding energies of C1s, O1s, and Ca2p. A monochromatic aluminum X-ray (Al Kα monochromatic; 1486.6 eV) was used as an XPS excitation source.

2.3. Coagulation and Adsorption Experiments

The kinetics of coagulation by two coagulants (i.e., $Ca(OH)_2$ and PACl) and adsorption by five adsorbents (i.e., aerobic granular sludge, AS, PAC, GAC, and zeolite due to its high ion-exchange capacity and low cost [33,34]) were investigated following the standard jar-test technique for TDS removal at pH 7. The pH of the ROC was adjusted to 7 using 0.001–0.1 M H_2SO_4 and NaOH solutions. The following jar-test ROC coagulation procedure was followed [35]: in each test, four different dosages (0.25, 0.50, 0.75 and 1.00 g/L) of each coagulant were added to 2 L of the pH-adjusted ROC sample in a C-JT tester (Changshin Science Co. Ltd., Busan, Korea) which were 2.4 L acrylic reactors equipped with six paddles. For effective mixing, the different coagulants and sorbents were injected near the stirring paddles using a pipette tip [36]. The sample was first mixed rapidly for 1 min at 400 rpm, followed by slow stirring for 6 h at 150 rpm in order to simulate the full-scale SBR process (1 cycle of 4 h of aerobic reaction, 1 h of sedimentation, 0.5 h of withdrawing, and 0.5 h of filling) [37,38].

Samples were collected at predetermined time intervals and filtered through a 0.45 μm membrane filter (Millipore Co., Bedford, MA, USA) to analyze the TDS concentration. The values of TDS (mg/L) were calculated by drying the filtrate at 105 °C overnight and then weighing the dried solids [39].

To investigate the underlying TDS biosorption mechanism by the aerobic granular sludge, the Lagergren first-order [40] and pseudo-second-order kinetic models [41] were employed, which can be expressed by Equations (1) and (2), respectively.

$$\frac{dq_t}{dt} = k_1(q_e - q_t) \tag{1}$$

$$q_t = \frac{k_2\, q_e^2\, t}{1 + k_2\, q_e\, t} \tag{2}$$

where q_t is the amount of TDS sorbed at time t (mg/g); k_1 and k_2 are the pseudo-first-order and pseudo-second-order rate constants for the biosorption process (1/h); q_e is the amount of TDS-adsorbed at equilibrium (mg/g); C_0 is the initial TDS concentration in the sample (mg/L); C_t is the liquid-phase TDS concentration at time t (mg/L); V is the volume of the sample (L); and M is the mass of the sorbent used (g).

After definite integration with the boundary conditions of $q_t = 0$ at $t = 0$ and $q_t = q_t$ at $t = t$, Equation (1) yields the linearized form (Equation (3)) as follows:

$$\log(q_e - q_t) = \log\, q_e - \frac{k_1 t}{2.303} \tag{3}$$

Equation (2) can be rearranged to obtain a linear form of

$$\frac{1}{q_t} = \frac{1}{k_2\, q_e^2} \cdot \frac{1}{t} + \frac{1}{q_e} \tag{4}$$

The amounts of TDS sorbed onto aerobic granular sludge were calculated as follows:

$$q_t = \frac{V(C_0 - C_t)}{M} \tag{5}$$

3. Results and Discussion

3.1. Characterization of Aerobic Granular Sludge

After 24 h of incubation in the SBR, the aerobic granular sludge sample was analyzed by SEM and TEM. Figure 2a,b show that the aerobic granular sludge had a compact and even surface surrounded by a biofilm of heterotrophic bacteria with extracellular polymeric substances (EPS). The XPS survey scan of the bare aerobic granular sludge (Figure 2c) shows that C, O, and Ca are the main surface elements. The XPS peaks at 286.2 eV, 347.7 eV, 438.0 eV, and 530.8 eV belong to C1s, Ca2p$_{3/2}$, Ca2s, and O1s, respectively [42]. The spatial distribution of EPS was determined using the fluorescent intensity data from CLSM microscopy with multiple fluorescent stains, as shown in Figure 2d–j. The EPS are considered to be high MW mixtures (containing proteins, polysaccharides, nucleic acids, and lipids) created by the lysis of microorganismal cells, which tend to adhere to the cell surfaces and enhance protection against an unfavorable external environment [43,44]. The concentration and composition of EPS may differ under different growth conditions that determine the internal cohesive or adhesive strengths. Protein was distributed evenly throughout the aerobic granular sludge, while α-D-glucopyranose polysaccharide accumulated at the outer layer of the granule. This result is consistent with observations by McSwain et al. [31].
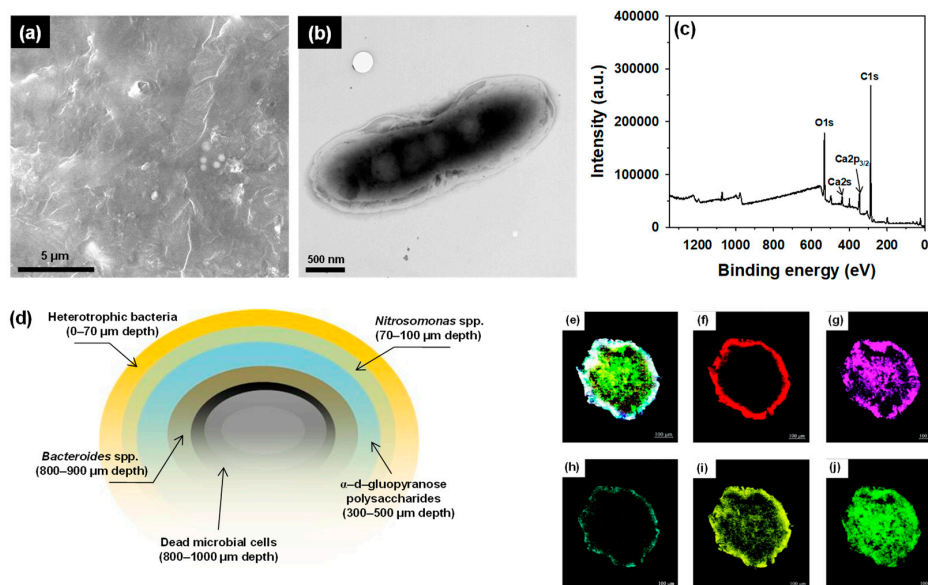
Figure 2. (**a**) SEM image; (**b**) TEM micrograph; and (**c**) X-ray photoelectron spectra of a wide survey scan of aerobic granular sludge; (**d**) The spatial distribution and vertical profile of extracellular polymeric substances (EPS) with depth in the aerobic granular sludge cultivated from the SBR reactor. CLSM images of aerobic granular sludge: (**e**) combined; (**f**) red: nucleic acid (SYTO 63); (**g**) pink: dead cells (SYTO blue); (**h**) light blue: α-D-glucopyranose polysaccharide (Con A); (**i**) yellow: lipid (Nile red); and (**j**) green: protein (FITC).

The BET surface areas of the coagulants and adsorbents used in this study were obtained from the nitrogen adsorption—desorption isotherms. Among the seven coagulants and adsorbents, aerobic granular sludge had the highest specific surface area (828.76 m^2/g), while the surface areas of Ca(OH)$_2$, PACl, AS, PAC, GAC, and zeolite were 267.34, 211.32, 654.44, 562.82, 484.83 and 362.54 m^2/g, respectively. This suggests that the use of aerobic granular sludge may achieve the highest TDS removal efficiency from ROC as the number of active sites available for TDS adsorption is highly dependent on the effective surface area of the coagulants/adsorbents [45].

3.2. Removal of TDS by Biosorption onto Aerobic Granular Sludge

Figure 3a shows the results of removing TDS from ROC by biosorption with aerobic granular sludge at pH 7. Influent TDS concentrations ranging from 2006 to 2017 mg/L were considered in this experiment. TDS sorption onto aerobic granular sludge achieved 13%, 30%, 41%, and 52% of the TDS removal efficiencies at aerobic granular sludge dosages of 0.25, 0.50, 0.75, and 1.0 g/L. At a dosage of 1 g/L, TDS removal capacity of an aerobic granular sludge dosage was higher than other coagulants and adsorbents studied (Ca(OH)$_2$: 25%, PACl: 6%, AS: 32%, PAC: 36%, GAC: 33%, and zeolite: 15% (described below)). However, TDS removal was less than 50% at an aerobic granular sludge dosage of <1 g/L. An increase in the concentration of aerobic granular sludge from 0.25 to 1.00 g/L enhanced the biosorption of TDS removal. This indicates that further treatments are indispensable for complete TDS reaction. Even though an aerobic granular sludge dosage of 1 g/L exhibited the enhanced TDS removal efficiency, further study is necessary to examine the treatability of higher concentrated TDS by biosorption onto aerobic granular in order to extend its applicability to high salinity water (~35,000 mg/L) [46]. During the 6 h reaction, TDS removal kinetics from ROC could be fitted to the pseudo-first-order kinetic model with a coefficient of determination (r^2) exceeding 0.95, which can be expressed by Equation (6) as follows:

$$-\ln\left(\frac{C}{C_0}\right) = kt \tag{6}$$

The pseudo-first-order rate constants (k) were calculated to be 0.027, 0.055, 0.087, and 0.125 h^{-1} for 0.25, 0.50, 0.75, and 1 g/L dosages of aerobic granular sludge, respectively.

The model lines in Figure 3b were obtained by plotting $\log(q_e - q_t)$ against t for different aerobic granular sludge dosages according to the linearized form of Lagergren first-order kinetic model (Equation (3)). The model parameters of Lagergren first-order and pseudo-second-order kinetics are summarized in Table 2.
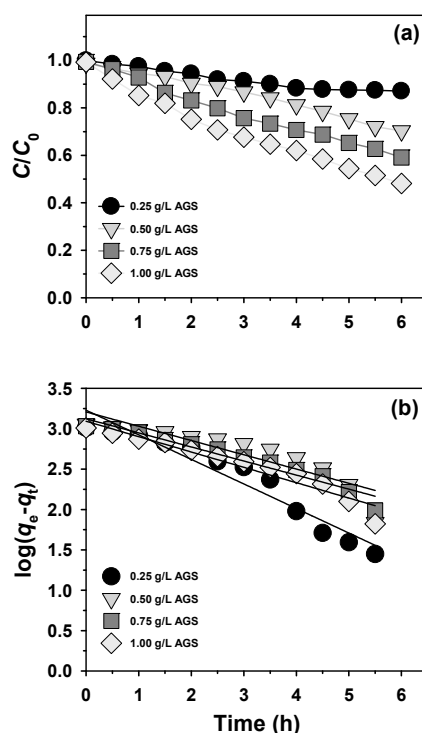

Figure 3. (**a**) TDS removal from ROC by adsorption using aerobic granular sludge; (**b**) Pseudo-first-order kinetic model for adsorption of TDS from ROC onto aerobic granular sludge. Experimental conditions: Influent TDS = 2006–2017 mg/L; [Aerobic granular sludge]$_0$ = 0.25, 0.50, 0.75, and 1.0 g/L; and pH 7.

Table 2. Parameters of the pseudo-first-order and second-order kinetic models for the TDS adsorption on the aerobic granular sludge at pH 7.

Aerobic Granular Sludge (g/L)	Exp	Pseudo-First-Order Kinetic			Pseudo-Second-Order Kinetic		
	$q_{e,exp}$ (mg/g)	k_1 (1/h)	$q_{e,cal1}$ (mg/g)	r^2	k_2 (1/h)	$q_{e,cal2}$ (mg/g)	r^2
0.25	1037	0.70	1698	0.962	0.94	3333	0.940
0.50	1190	0.31	1369	0.979	0.97	1667	0.965
0.75	1094	0.40	1330	0.990	0.97	3333	0.969
1.0	1040	0.44	1240	0.993	0.99	2000	0.985

For 0.25–1.0 g/L of aerobic granular sludge dosage, the correlation coefficient values (r^2) obtained from the Lagergren first-order model (0.962–0.993) were higher than those calculated from the pseudo-second-order kinetic model (0.940–0.985). This suggested that the TDS biosorption process was preferably described by the Lagergren first-order model. According to the Lagergren first-order model assumption, one dissolved solid molecule was sorbed onto one sorption site on the surface of the aerobic granular sludge, and the diffusion of the TDS dominated the adsorption velocity [47,48]. The pseudo-second-order kinetic model could not fit the experimental data due to a disparity with the rate-limiting chemisorption mechanism. The k_1 and q_e values calculated from the slopes and intercepts of the linear plots of the Lagergren first-order equation for the sorption model were $k_1 = 0.70$,

0.31, 0.40, and 0.44 h^{-1}, and q_e = 1698, 1369, 1330, and 1240 mg/g for 0.25, 0.50, 0.75, and 1.0 g/L of aerobic granular sludge, respectively. The calculated q_e values were higher than those obtained from the experiments, suggesting that the Lagergren first-order model is suitable for the biosorption of TDS onto the aerobic granular sludge, and further TDS removal could be expected over a longer time period.

3.3. Comparison of TDS Removal by Different Coagulants and Adsorbents

A comparative study of the removal of TDS (influent concentrations of 2000−2033 mg/L) by six different coagulants and adsorbents (i.e., Ca(OH)$_2$, PACl, AS, PAC, GAC, and zeolite) was conducted under constant conditions. The results are presented in Figure 4. An increase in coagulant/adsorbent dosage from 0.25 to 1.00 g/L enhanced TDS removal during 6 h of reaction. The TDS removal efficiency at 1.0 g/L of coagulants/adsorbents under optimal conditions decreased in the following order: PAC (36%) > GAC (33%) > AS (32%) > Ca(OH)$_2$ (25%) > zeolite (15%) > PACl (6%), with *k* values of 0.09, 0.08, 0.06, 0.04, 0.02, and 0.01 h^{-1} (r^2 = 0.91–0.97), respectively, according to the pseudo-first-order kinetic model. This indicates that the TDS removal efficiency by those coagulants/adsorbents in the same concentration range was below 50%, which demonstrates that aerobic granular sludge had higher removal activity than other substances. This could be because it had the highest specific surface area (828.76 m^2/g), providing a greater number of active sites for TDS adsorption.

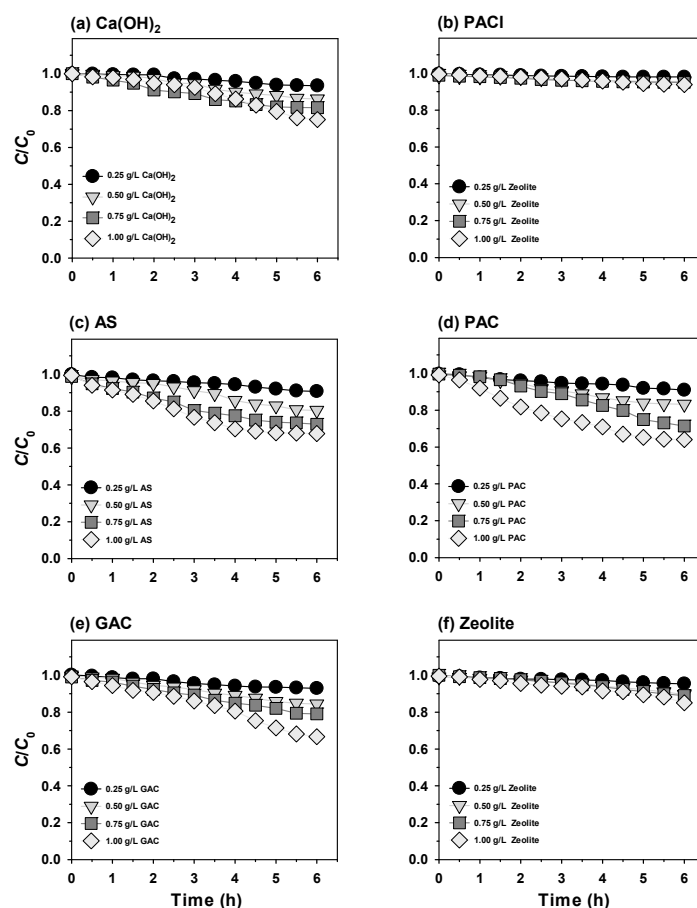**Figure 4.** TDS removal from ROC by coagulation using (**a**) Ca(OH)$_2$ and (**b**) PACl, and adsorption using (**c**) AS; (**d**) PAC; (**e**) GAC; and (**f**) zeolite. Experimental conditions: Influent TDS = 2000–2033 mg/L; [Ca(OH)$_2$]$_0$ = [PACl]$_0$ = [AS]$_0$ = [PAC]$_0$ = [GAC]$_0$ = [zeolite]$_0$ = 0.25 g/L, 0.50 g/L, 0.75 g/L, and 1.00 g/L; and pH 7.

3.4. TDS Removal Mechanism by Biosorption onto Aerobic Granular Sludge

Figure 5 presents the SEM and TEM images of TDS-sorbed aerobic granular sludge at different TDS concentrations (2000–4000 mg/L). A layer of biofilm was attached to the outer surface of the aerobic granular sludge. Microscopic examination revealed sharp edge crystals on the surface of the aerobic granular sludge as TDS concentrations increased. The biofilm on the aerobic granular sludge is directly linked to EPS because TDS adsorption is strongly dependent on the type of EPS. The compositions and physicochemical properties of EPS vary during synthesis from sludge (such as polyanionic, neutral, or polycationic) [49]. As TDS removal by aerobic granular sludge was considerably higher than that observed for the other six coagulants and adsorbents, it was important to consider the biosorption process during ROC pretreatment.
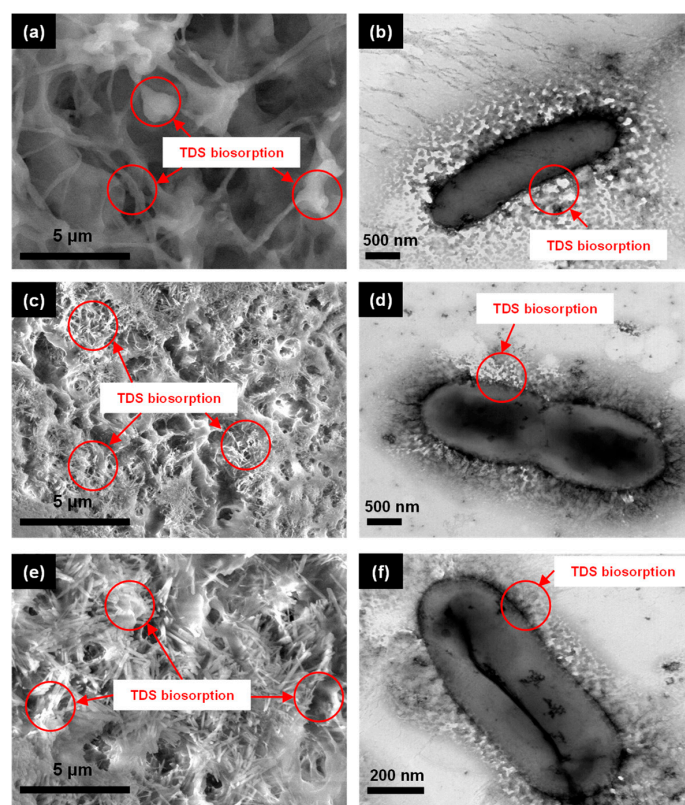

Figure 5. SEM images of TDS-sorbed aerobic granular sludge at TDS concentrations of (**a**) 2000 mg/L; (**c**) 3000 mg/L; and (**e**) 4000 mg/L; TEM micrographs of TDS-sorbed aerobic granular sludge at TDS concentrations of (**b**) 2000 mg/L; (**d**) 3000 mg/L; and (**f**) 4000 mg/L. Experimental conditions: [Aerobic granular sludge]$_0$ = 1.0 g/L; and pH 7.

XPS analysis of aerobic granular sludge that had been exposed to 2000, 3000, and 4000 mg/L of TDS for 6 h was also conducted to identify the constituent elements of the sample (Figure 6). The wide XPS survey scans show similar peak positions of carbon and oxygen to those of the bare aerobic granular sludge (Figure 2c). The relative atomic XPS percentage (at.%) of C1s decreased significantly to 12.7%, 22.8%, and 18.9% for TDS concentrations of 2000, 3000, and 4000 mg/L, respectively. Similarly, the O1s peak at 530.8 eV, corresponding to O^{2-} in a lattice, was weaker (69.2%, 81.2%, and 91.9% for TDS concentrations of 2000, 3000, and 4000 mg/L, respectively) than that of the bare aerobic granular sludge. However, the O1s peak slightly increased as the TDS concentration increased from 2000 to 4000 mg/L. The O1s/C1s peak ratio calculated from the XPS survey scan thus increased after the biosorption of the TDS on the aerobic granular sludge, which indicates a partial oxidation of the TDS-sorbed aerobic granular sludge samples. The peak at 347.7 eV, which corresponds to Ca2p$_{3/2}$,

significantly increased for TDS-sorbed aerobic granular sludge (27.0 at.%, 20.9 at.%, and 26.6 at.% for TDS concentrations of 2000, 3000, and 4000 mg/L, respectively). In addition, a more prominent XPS peak was observed at 438.0 eV, corresponding to Ca2s in TDS-sorbed aerobic granular sludge. Previous research reported that EPS and Ca(II) ions plays an important role in adsorption of heavy metal ions on the aerobic granules. Wang et al. [50] showed that the disintegrated aerobic granules had 2.34 times greater adsorption capacity of EPS than pristine aerobic granules, which enhanced Cu(II) biosorption capacity. Wei et al. [51] reported that EPS strongly engaged in the sorption process between Zn(II) and the aerobic granular sludge. Kim et al. [52] reported that Ca(II) ions (302 ± 54.7 mg/L) in the influent act as the bridges between the negatively charged active sites of microorganisms and EPS. Ca(II) ions were also promoted to increase the size of aerobic granular sludge by enhancing the production of polysaccharides, which played a significant role in increasing the adhesion forces between the microorganism aggregates [53]. Thus, the XPS analysis results indicated that the removal of TDS by the aerobic granular sludge resulted from a bridging role of Ca(II) ions between TDS and aerobic granular sludge.
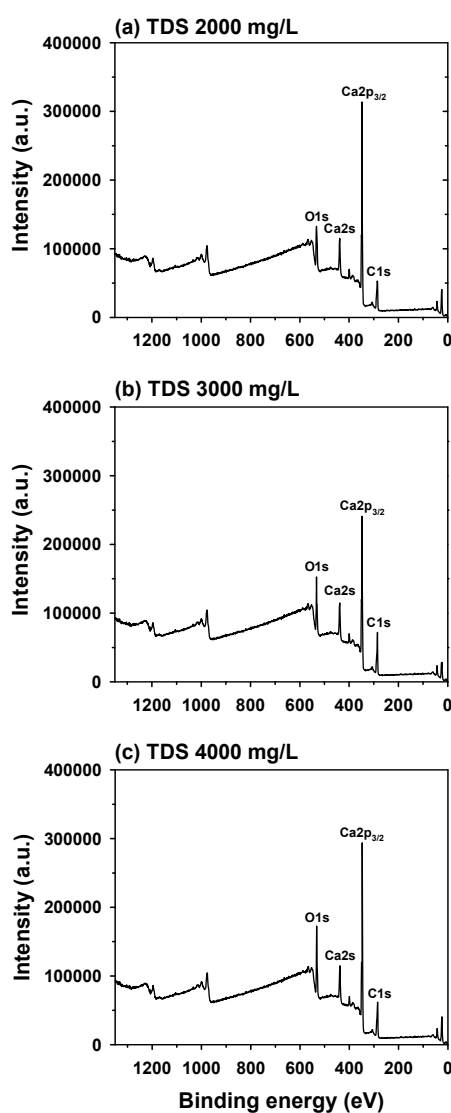

Figure 6. X-ray photoelectron spectra of wide survey scan of TDS-sorbed aerobic granular sludge at TDS concentrations of (**a**) 2000 mg/L, (**b**) 3000 mg/L, and (**c**) 4000 mg/L. Experimental conditions: [Aerobic granular sludge]$_0$ = 1.0 g/L, and pH 7.

4. Conclusions

The aerobic granular sludge was evaluated as a novel biosorbent for their removal capacity of TDS in ROC from a municipal wastewater reclamation plant. The removal efficiencies of TDS by various coagulant and adsorbent materials (i.e., Ca(OH)$_2$, PACl, AS, PAC, GAC, and zeolite) were also compared by varying the dosage of the coagulant/adsorbent. SEM, TEM, and XPS analysis showed that TDS was extensively attached to the aerobic granular sludge after biosorption. The results showed that TDS removal by aerobic granular sludge was considerably higher than that by the other coagulants and adsorbents. The kinetic experiments revealed that the removal of TDS was more rapid with a higher dosage of aerobic granular sludge in ROC. The biosorption of the TDS on aerobic granular sludge follows the Lagergren first-order model, and the highest TDS biosorption capacity was calculated to be 1698 mg/g. This regenerable biosorbent could be a potential alternative in the pretreatment of ROC for biological nitrogen removal in a membrane bioreactor (MBR). Further research should be conducted to better understand the effect of pH on the TDS removal efficiency by biosorption, reusability of aerobic granular sludge using ion exchange, or the desorption of the used granules, and the nitrogen removal efficiency of a MBR system receiving effluent from the proposed biosorption process.

Abbreviations

RO	reverse osmosis
ROC	reverse osmosis concentrates
TDS	total dissolved solids
MSF	multi-stage flash
EfOM	effluent organic matter
ZLD	zero liquid discharge
HERO^{TM}	high-efficiency reverse osmosis
MBR	membrane bioreactor
DOC	dissolved organic carbon
GAC	granular activated carbon
PACl	polyaluminum chloride
AS	activated sludge
PAC	powdered activated carbon
SBR	sequencing batch reactor
DI	deionized
FITC	fluorescein isothiocyanate
CLSM	confocal laser scanning microscopy
BET	Brunauer-Emmett-Teller
SEM	scanning electron microscope
TEM	transmission electron microscope
XPS	X-ray photoelectron spectroscopy
EPS	extracellular polymeric substances

References

1.　Mohammadi, T.; Kaviani, A. Water shortage and seawater desalination by electrodialysis. *Desalination* **2003**, *158*, 267–270. [CrossRef]

2.　World Health Organization (WHO); UNICEF. *Global Water Supply and Sanitation Assessment 2000 Report*; WHO: Geneva, Switzerland, 2000.

3.　Seckler, D.; Barker, R.; Amarasinghe, U. Water scarcity in the twenty-first century. *Int. J. Water Resour. Dev.* **1999**, *15*, 29–42. [CrossRef]

4.　Urdea, M.; Penny, L.A.; Olmsted, S.S.; Giovanni, M.Y.; Kaspar, P.; Shepherd, A.; Wilson, P.; Dahl, C.A.; Buchsbaum, S.; Moeller, G. Requirements for high impact diagnostics in the developing world. *Nature* **2006**, *444*, 73–79. [CrossRef] [PubMed]

5.　Ryabtsev, A.; Kotsupalo, N.; Titarenko, V.; Igumenov, I.; Gelfond, N.; Fedotova, N.; Morozova, N.; Shipachev, V.; Tibilov, A. Development of a two-stage electrodialysis set-up for economical desalination of sea-type artesian and surface waters. *Desalination* **2001**, *137*, 207–214. [CrossRef]

6.　Cath, T.Y.; Childress, A.E.; Elimelech, M. Forward osmosis: Principles, applications, and recent developments. *J. Membr. Sci.* **2006**, *281*, 70–87. [CrossRef]

7.　Xiao, D.; Tang, C.Y.; Zhang, J.; Lay, W.C.; Wang, R.; Fane, A.G. Modeling salt accumulation in osmotic membrane bioreactors: Implications for FO membrane selection and system operation. *J. Membr. Sci.* **2011**, *366*, 314–324. [CrossRef]

8.　Chelme-Ayala, P.; Smith, D.W.; El-Din, M.G. Membrane concentrate management options: A comprehensive critical review. *J. Environ. Eng. Sci.* **2009**, *8*, 326–339. [CrossRef]

9.　Fritzmann, C.; Löwenberg, J.; Wintgens, T.; Melin, T. State-of-the-art of reverse osmosis desalination. *Desalination* **2007**, *216*, 1–76. [CrossRef]

10.　Buros, O.K. *The ABCs of Desalting*; International Desalination Association: Topsfield, MA, USA, 2000.

11.　Al-Rifai, J.H.; Gabelish, C.L.; Schäfer, A.I. Occurrence of pharmaceutically active and non-steroidal estrogenic compounds in three different wastewater recycling schemes in Australia. *Chemosphere* **2007**, *69*, 803–815. [CrossRef] [PubMed]

12.　Pehlivanoglu-Mantas, E.; Sedlak, D.L. Wastewater-derived dissolved organic nitrogen: Analytical methods, characterization, and effects—A review. *Crit. Rev. Environ. Sci. Technol.* **2006**, *36*, 261–285. [CrossRef]

13.　Bellona, C.; Drewes, J.E.; Xu, P.; Amy, G. Factors affecting the rejection of organic solutes during NF/RO treatment—A literature review. *Water Res.* **2004**, *38*, 2795–2809. [CrossRef] [PubMed]

14.　Bond, R.; Veerapaneni, S. *Zero Liquid Discharge and Volume Minimization for Inland Desalination*; American Water Works Association Research Foundation Project #3010; American Water Works Association Research Foundation: Las Vegas, NV, USA, 2000.

15.　Jordahl, J. *Beneficial and Nontraditional Uses of Concentrate*; Water Reuse Foundation: Alexandria, VA, USA, 2006.

16.　Bagastyo, A.Y.; Keller, J.; Poussade, Y.; Batstone, D.J. Characterisation and removal of recalcitrants in reverse osmosis concentrates from water reclamation plants. *Water Res.* **2011**, *45*, 2415–2427. [CrossRef] [PubMed]

17.　Zhou, T.; Lim, T.-T.; Chin, S.-S.; Fane, A. Treatment of organics in reverse osmosis concentrate from a municipal wastewater reclamation plant: Feasibility test of advanced oxidation processes with/without pretreatment. *Chem. Eng. J.* **2011**, *166*, 932–939. [CrossRef]

18.　Dialynas, E.; Mantzavinos, D.; Diamadopoulos, E. Advanced treatment of the reverse osmosis concentrate produced during reclamation of municipal wastewater. *Water Res.* **2008**, *42*, 4603–4608. [CrossRef] [PubMed]

19.　Gur-Reznik, S.; Katz, I.; Dosoretz, C.G. Removal of dissolved organic matter by granular-activated carbon adsorption as a pretreatment to reverse osmosis of membrane bioreactor effluents. *Water Res.* **2008**, *42*, 1595–1605. [CrossRef] [PubMed]

20.　Jiang, H.L.; Tay, J.H.; Tay, S.L. Aggregation of immobilized activated sludge cells into aerobically grown microbial granules for the aerobic biodegradation of phenol. *Lett. Appl. Microbiol.* **2002**, *35*, 439–445. [CrossRef] [PubMed]

21.　Moy, B.P.; Tay, J.H.; Toh, S.K.; Liu, Y.; Tay, S.L. High organic loading influences the physical characteristics of aerobic sludge granules. *Lett. Appl. Microbiol.* **2002**, *34*, 407–412. [CrossRef] [PubMed]

22.　Adav, S.S.; Chang, C.H.; Lee, D.J. Hydraulic characteristics of aerobic granules using size exclusion chromatography. *Biotechnol. Bioeng.* **2008**, *99*, 791–799. [CrossRef] [PubMed]

23. Bassin, J.; Pronk, M.; Kraan, R.; Kleerebezem, R.; Van Loosdrecht, M. Ammonium adsorption in aerobic granular sludge, activated sludge and anammox granules. *Water Res.* **2011**, *45*, 5257–5265. [CrossRef] [PubMed]

24. Liu, Y.; Yang, S.-F.; Xu, H.; Woon, K.-H.; Lin, Y.-M.; Tay, J.-H. Biosorption kinetics of cadmium(II) on aerobic granular sludge. *Process Biochem.* **2003**, *38*, 997–1001. [CrossRef]

25. Adav, S.S.; Lee, D.-J.; Show, K.-Y.; Tay, J.-H. Aerobic granular sludge: Recent advances. *Biotechnol. Adv.* **2008**, *26*, 411–423. [CrossRef] [PubMed]

26. Wang, Q.; Du, G.; Chen, J. Aerobic granular sludge cultivated under the selective pressure as a driving force. *Process Biochem.* **2004**, *39*, 557–563. [CrossRef]

27. Chen, M.; Lee, D.; Tay, J. Distribution of extracellular polymeric substances in aerobic granules. *Appl. Microbiol. Biotechnol.* **2007**, *73*, 1463–1469. [CrossRef] [PubMed]

28. Chen, M.-Y.; Lee, D.-J.; Tay, J.-H.; Show, K.-Y. Staining of extracellular polymeric substances and cells in bioaggregates. *Appl. Microbiol. Biotechnol.* **2007**, *75*, 467–474. [CrossRef] [PubMed]

29. Li, L.-L.; Tong, Z.-H.; Fang, C.-Y.; Chu, J.; Yu, H.-Q. Response of anaerobic granular sludge to single-wall carbon nanotube exposure. *Water Res.* **2015**, *70*, 1–8. [CrossRef] [PubMed]

30. Adav, S.S.; Lee, D.-J.; Tay, J.-H. Extracellular polymeric substances and structural stability of aerobic granule. *Water Res.* **2008**, *42*, 1644–1650. [CrossRef] [PubMed]

31. McSwain, B.; Irvine, R.; Hausner, M.; Wilderer, P. Composition and distribution of extracellular polymeric substances in aerobic flocs and granular sludge. *Appl. Environ. Microbiol.* **2005**, *71*, 1051–1057. [CrossRef] [PubMed]

32. Barrett, E.P.; Joyner, L.G.; Halenda, P.P. The determination of pore volume and area distributions in porous substances. I. Computations from nitrogen isotherms. *J. Am. Chem. Soc.* **1951**, *73*, 373–380. [CrossRef]

33. Alver, E.; Metin, A.Ü. Anionic dye removal from aqueous solutions using modified zeolite: Adsorption kinetics and isotherm studies. *Chem. Eng. J.* **2012**, *200*, 59–67. [CrossRef]

34. Crini, G. Non-conventional low-cost adsorbents for dye removal: A review. *Bioresour. Technol.* **2006**, *97*, 1061–1085. [CrossRef] [PubMed]

35. Wang, Y.; Han, T.; Xu, Z.; Bao, G.; Zhu, T. Optimization of phosphorus removal from secondary effluent using simplex method in Tianjin, China. *J. Hazard. Mater.* **2005**, *121*, 183–186. [CrossRef] [PubMed]

36. Lee, W.; Westerhoff, P. Dissolved organic nitrogen removal during water treatment by aluminum sulfate and cationic polymer coagulation. *Water Res.* **2006**, *40*, 3767–3774. [CrossRef] [PubMed]

37. Oselame, M.; Fernandes, H.; Costa, R. Simulation and calibration of a full-scale sequencing batch reactor for wastewater treatment. *Braz. J. Chem. Eng.* **2014**, *31*, 649–658. [CrossRef]

38. Li, T.; Zhu, Z.; Wang, D.; Yao, C.; Tang, H. Characterization of floc size, strength and structure under various coagulation mechanisms. *Powder Technol.* **2006**, *168*, 104–110. [CrossRef]

39. Thomas, L.P.; Marino, B.M.; Szupiany, R.N.; Gallo, M. Characterisation of the suspended particulate matter in a stratified estuarine environment employing complementary techniques. *Cont. Shelf Res.* **2017**, *148*, 37–43. [CrossRef]

40. Lagergren, S. Zur theorie der sogenannten adsorption geloster stoffe. Kungliga svenska vetenskapsakademiens. *Handlingar* **1898**, *24*, 1–39.

41. Ho, Y.-S.; McKay, G. Pseudo-second order model for sorption processes. *Process Biochem.* **1999**, *34*, 451–465. [CrossRef]

42. Dhankhar, S.; Bhalerao, G.; Ganesamoorthy, S.; Baskar, K.; Singh, S. Growth and comparison of single crystals and polycrystalline brownmillerite $Ca_2Fe_2O_5$. *J. Cryst. Growth* **2017**, *468*, 311–315. [CrossRef]

43. Sheng, G.-P.; Yu, H.-Q.; Li, X.-Y. Extracellular polymeric substances (EPS) of microbial aggregates in biological wastewater treatment systems: A review. *Biotechnol. Adv.* **2010**, *28*, 882–894. [CrossRef] [PubMed]

44. Ahimou, F.; Semmens, M.J.; Haugstad, G.; Novak, P.J. Effect of protein, polysaccharide, and oxygen concentration profiles on biofilm cohesiveness. *Appl. Environ. Microbiol.* **2007**, *73*, 2905–2910. [CrossRef] [PubMed]

45. Xu, Y.-H.; Nakajima, T.; Ohki, A. Adsorption and removal of arsenic(V) from drinking water by aluminum-loaded Shirasu-zeolite. *J. Hazard. Mater.* **2002**, *92*, 275–287. [CrossRef]

46. El-Manharawy, S.; Hafez, A. Water type and guidelines for RO system design. *Desalination* **2001**, *139*, 97–113. [CrossRef]

47. Boparai, H.K.; Joseph, M.; O'Carroll, D.M. Kinetics and thermodynamics of cadmium ion removal by adsorption onto nano zerovalent iron particles. *J. Hazard. Mater.* **2011**, *186*, 458–465. [CrossRef] [PubMed]

48. Zhou, N.; Chen, H.; Xi, J.; Yao, D.; Zhou, Z.; Tian, Y.; Lu, X. Biochars with excellent Pb(II) adsorption property produced from fresh and dehydrated banana peels via hydrothermal carbonization. *Bioresour. Technol.* **2017**, *232*, 204–210. [CrossRef] [PubMed]

49. Sutherland, I.W. Biofilm exopolysaccharides: A strong and sticky framework. *Microbiology* **2001**, *147*, 3–9. [CrossRef] [PubMed]

50. Wang, X.-H.; Song, R.-H.; Teng, S.-X.; Gao, M.-M.; Ni, J.-Y.; Liu, F.-F.; Wang, S.-G.; Gao, B.-Y. Characteristics and mechanisms of Cu(II) biosorption by disintegrated aerobic granules. *J. Hazard. Mater.* **2010**, *179*, 431–437. [CrossRef] [PubMed]

51. Wei, D.; Li, M.; Wang, X.; Han, F.; Li, L.; Guo, J.; Ai, L.; Fang, L.; Liu, L.; Du, B. Extracellular polymeric substances for Zn(II) binding during its sorption process onto aerobic granular sludge. *J. Hazard. Mater.* **2016**, *301*, 407–415. [CrossRef] [PubMed]

52. Kim, H.G.; Kim, S.S.; Kim, S.C.; Joo, H.J. Effects of Ca^{2+} on biological nitrogen removal in reverse osmosis concentrate and adsorption treatment. *J. Ind. Eng. Chem.* **2018**, *57*, 216–225. [CrossRef]

53. Tay, S.T.-L.; Moy, B.Y.-P.; Jiang, H.-L.; Tay, J.-H. Rapid cultivation of stable aerobic phenol-degrading granules using acetate-fed granules as microbial seed. *J. Biotechnol.* **2005**, *115*, 387–395. [CrossRef] [PubMed]